Journal of Statistical Physics, Vol. 63, Nos. 5/6, 1991

Theory of Percolation in Fluids of Long Molecules

Kevin Leung[1] and David Chandler[1]

Received February 14, 1991

We use the reference interaction site model (RISM) integral equation theory to study the percolation behavior of fluids composed of long molecules. We examine the roles of hard core size and of length-to-width ratio on the percolation threshold. The critical density ρ_c is a nonmonotonic function of these parameters exhibiting competition of different effects. Comparisons with Monte Carlo calculations of others are reasonably good. For critical exponents, the theory yields $\gamma = 2\nu = 2$ for molecules of any noninfinite length L. When L is very large, the theory yields $\rho_c \sim L^{-2}$. These predictions compare favorably with observations of the conductivity for random assemblies of conductive fibers. The threshold region where asymptotic scaling holds requires the correlation length $\xi \sim (\delta\rho/\rho_c)^{-\nu}$ to be much larger than L. Evidently, the range of densities in this region diminishes as L increases, requiring that density deviations from ρ_c be no larger than $\delta\rho \sim L^{-2}$. Otherwise, crossover behavior will be observed.

KEY WORDS: Percolation; RISM integral equation.

1. INTRODUCTION

Many phenomena which occur in disordered systems can be understood in terms of the connectivity and clustering of particles. Higher densities increase the tendency of particles to cluster together. At the critical percolation density ρ_c, which is in general dependent upon temperature and microscopic details, a macroscopic cluster appears, spanning the entire system. This sharp geometric phase transition is the percolation transition (see, e.g., ref. 1). It is often accompanied by drastic changes in the physical properties of the system. The sol–gel transition and the insulator–conductor transition in composite materials can be two such examples. For fluid

[1] Department of Chemistry, University of California, Berkeley, California 94720.

822/63/5-6-3

systems, the effects of anisotropy, intermolecular correlations, and density fluctuations seem best described by continuous percolation rather than by lattice models. In this paper we apply a version of the reference interaction site method (RISM) to examine the roles of molecular shape and excluded volume on the percolation transitions in fluids.

The Ornstein–Zernike integral equation approach to continuum percolation[2] and its solution within the Percus–Yevick[8] approximation were introduced by Coniglio *et al.*[2] Chiew and Glandt[3] applied this method to calculate among other things the critical densities of permeable-sphere models. Chiew and Stell[4] improved upon this approximation with a type of generalized mean spherical approximation.[9] Stratt and co-workers[5] seem to have been the first to implement these types of integral equations with proper account for excluded volume, and they predicted trends that are in qualitative agreement with Monte Carlo calculations.[10,11] Lupkowski and Monson[12] and Laria and Vericat[13] extended this approach to treat fluids composed of nonspherical particles by employing the interaction site formalism of Chandler and co-workers (see refs 14 for reviews). Our work described herein rests upon the contributions of Lupkowski and Monson and of Laria and Vericat. Excluded-volume effects, which generally dominate the intermolecular structure of liquids,[15] were not directly taken into account by these workers. Nor did they consider extremely long molecules. Others have considered percolation with very long molecules (see, e.g., refs. 16), but often employed approximations that can be improved upon with the RISM approach. The present paper will address both the effects of excluded volume and long molecular lengths.

Further extensions to study the role of attractive particle–particle interactions or the presence of more than one species are clearly feasible. Such extension have been carried out, for example, by Xu and Stell[6] and by Chiew *et al.*,[7] respectively, for spheres, but these apparent extensions are not the focus of this paper.

The remainder of this paper is organized as follows. In Section 2 we review the pertinent interaction-site equations and specify the model we are using. The molecular size and shape dependence of ρ_c and the critical behavior near percolation determined from numerical solutions of RISM integral equations are examined in Section 3. The paper is concluded in Section 4 with a discussion containing analytical analysis and proposals for future work. An Appendix provides some details pertaining to our calculations that are omitted from the main text.

[2] Refs. 2–7 are representative but not inclusive of the large literature in this area.

2. FORMALISM AND MODEL

2.1. Correlation Functions

The central object in our studies is the site–site connectedness function, $h^+_{\alpha\gamma}(\mathbf{r}, \mathbf{r}')$, giving the probability density that site α of a molecule exists at $\mathbf{r}$ and site γ of another molecule in the same cluster exists at $\mathbf{r}'$. Two particles are in the same cluster if at least one site on one particle is directly connected to one site of the other, or if there exists a continuous path between them with direct connections forming the links in the path. The definition of "direct connectivity" utilizes the concept of physical clusters[17] (see below).

For an isotropic fluid of uniform density $\rho = \langle N/V \rangle$, $h^+_{\alpha\gamma}(\mathbf{r}, \mathbf{r}') = h^+_{\alpha\gamma}(|\mathbf{r} - \mathbf{r}'|)$, where

$$\rho^2 h^+_{\alpha\gamma}(r) = \sum_{i \neq j} \langle \delta(\mathbf{r}_i^{(\alpha)})\, \delta(\mathbf{r}_j^{(\gamma)} - \mathbf{r}) \rangle' \tag{2.1}$$

Here, as usual, $\mathbf{r}_i^{(\alpha)}$ denotes the position of site α in molecule i. The prime on the average indicates that in the ensemble, molecules i and j belong to the same physical cluster.

The mean cluster size S, which is one measure of the proximity to percolation, is given by

$$\begin{aligned} S &= 1 + \rho \int d\mathbf{r}\, h^+_{\alpha\gamma}(\mathbf{r}) \\ &= 1 + \rho \hat{h}^+_{\alpha\gamma}(0) \end{aligned} \tag{2.2}$$

where $\hat{h}^+_{\alpha\gamma}(k)$ denotes the spatial Fourier transform of $h^+_{\alpha\gamma}(r)$. As $k \to 0$, $\hat{h}^+_{\alpha\gamma}(k)$ is independent of the site labels, α and γ. This invariance is due to the constraint of stochiometry.

Another measure of the percolation threshold is the correlation length $\xi_{\alpha\gamma}$ defined as

$$\begin{aligned} \xi^2_{\alpha\gamma} &= \int d\mathbf{r}\, h^+_{\alpha\gamma}(r) r^2 \Big/ \hat{h}_{\alpha\gamma}(0) \\ &= \lim_{k \to 0} \{[-3/\hat{h}^+_{\alpha\gamma}(k)]\, d^2 \hat{h}^+_{\alpha\gamma}(k)/dk^2\} \end{aligned} \tag{2.3}$$

As the percolation transition is approached, S and $\xi_{\alpha\gamma}$ diverge. In that limit, $\xi_{\alpha\gamma}$ becomes independent of the site labels α and γ, i.e., $\xi_{\alpha\gamma} \to \xi$.

The divergences of S and ξ can be characterized by critical exponents γ and ν:

$$S \sim (\rho_c - \rho)^{-\gamma} \tag{2.4}$$

and

$$\xi \sim (\rho_c - \rho)^{-\nu} \tag{2.5}$$

In principle, for rigid molecules, the quantities ρ_c, γ, and ν could also be computed from $h^+(r, \mathbf{\Omega}_1, \mathbf{\Omega}_2)$, the orientation-dependent pair connectedness function. This correlation function may be useful for expressing formal results, but for calculations, we do not know how to make accurate estimates with it. In contrast, the interaction site formalism[14] is not limited to rigid molecular species, and it provides a computationally convenient route from which the site–site correlation functions *can* be accurately estimated.

2.2. Model and Connectivity

To analyze connectivity, one may follow Hill[17] in separating the Mayer cluster functions into bonding parts plus remainders. Specifically, let $f_{\alpha\gamma}(r)$ denote the site–site Mayer cluster function. Then

$$f_{\alpha\gamma}(r) = f^+_{\alpha\gamma}(r) + f^*_{\alpha\gamma}(r) \tag{2.6}$$

where $f^+_{\alpha\gamma}(r)$ is the bonding portion. This bonding cluster function is short ranged, being nonzero only where two sites are directly connected. The simplest form is the one we adopt herein,

$$\begin{aligned} f^+_{\alpha\gamma}(r) &= +1, \qquad \sigma < r < d \\ &= 0, \qquad r \geqslant d,\ r < \sigma \end{aligned} \tag{2.7}$$

Further, we consider herein only the simplest class of models for a molecular fluid, the one in which the site–site interactions are hard cores,

$$\begin{aligned} f_{\alpha\gamma}(r) &= -1, \qquad r < \sigma \\ &= 0, \qquad r \geqslant \sigma \end{aligned} \tag{2.8}$$

The M sites of a molecule are fused rigidly and equally spaced on a line of length

$$L = (M-1)l \tag{2.9}$$

as illustrated in Fig. 1.

The intramolecular bonding leads one to consider diagrammatic expansions involving intramolecular distributions such as

$$s_{\alpha\gamma}(r) = (1 - \delta_{\alpha\gamma}) \langle \delta(\mathbf{r} - \mathbf{r}_1^{(\alpha)} - \mathbf{r}_1^{(\gamma)}) \rangle \tag{2.10}$$

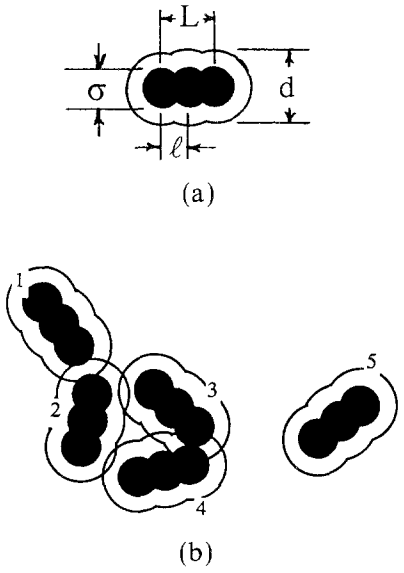

Fig. 1. (a) Sample molecule showing the meaning of the lengths L, l, σ, and d. (b) Molecules 1, 2, 3, and 4 all belong to the same cluster. Molecule 5 is not connected to any of the above.

as well as the intermolecular f-functions.[18] Connectivity in a physical cluster is then defined in terms of paths involving intermolecular $f^{+}_{\alpha\gamma}$-bonds and intramolecular s-bonds. Lupkowski and Monson[12] were the first to describe the interaction site cluster series (itself arising from a different sort of physical cluster analysis[19]) in this context.

2.3. RISM Equations

Useful approximations in the interaction site formalism are usually based on the Ornstein–Zernike-like equation

$$\mathbf{h}(r) = \boldsymbol{\omega} * \mathbf{c} * \boldsymbol{\omega}(r) + \rho\boldsymbol{\omega} * \mathbf{c} * \mathbf{h}(r) \tag{2.11}$$

introduced by Chandler and Andersen[20] and often called the RISM equation. Here, $\mathbf{h}(r)$ refers to the $M \times M$ matrix of site–site pair correlation functions $h_{\alpha\gamma}$, $\boldsymbol{\omega}(r)$ refers to the intramolecular correlation functions,

$$\omega_{\alpha\gamma}(r) = \delta_{\alpha\gamma}\,\delta(\mathbf{r}) + s_{\alpha\gamma}(r) \tag{2.12}$$

and $\mathbf{c}(r)$ is the matrix of the site–site direct correlation functions, $c_{\alpha\gamma}(r)$. The set of these latter auxiliary functions is defined by the Chandler–Andersen equation, (2.11).

Closures to Eq. (2.11) must provide a second independent connection between $\mathbf{h}(r)$ and $\mathbf{c}(r)$. The venerable Percus–Yevick closure,[8] adapted in this context, yields

$$c_{\alpha\gamma}(r) = f_{\alpha\gamma}(r)\, y_{\alpha\gamma}(r) \tag{2.13}$$

where $y_{\alpha\gamma}(r)$ is the "indirect" correlation function,

$$y_{\alpha\gamma}(r) = [1 + h_{\alpha\gamma}(r)]/[1 + f_{\alpha\gamma}(r)] \tag{2.14}$$

Equations (2.13) and (2.11) applied to simple hard-core molecules yield

$$\begin{aligned} h_{\alpha\gamma}(r) &= -1, \qquad r < \sigma \\ c_{\alpha\gamma}(r) &= 0, \qquad r > \sigma \end{aligned} \tag{2.15}$$

which is an often employed closure in the RISM theory.[14] We use it herein, too.

The interaction site diagrams summed by solving Eqs. (2.11) with (2.13) have been identified by Chandler.[21] As one possible approximation, Lupkowski and Monson[12] suggested the partitioning of Chandler's series into connected and disconnected parts. For the case of hard-core molecules, Eq. (2.8), with the bonding function (2.7), the partitioning leads to the following RISM integral equations describing the connectivity functions:

$$\mathbf{h}^+(r) = \boldsymbol{\omega} * \mathbf{c}^+ * \boldsymbol{\omega}(r) + \rho\boldsymbol{\omega} * \mathbf{c}^+ * \mathbf{h}^+(r) \tag{2.16}$$

with

$$\begin{aligned} h^+_{\alpha\gamma}(r) &= 0, \qquad r < \sigma \\ &= h_{\alpha\gamma}(r) + 1, \qquad \sigma < r < d \end{aligned} \tag{2.17}$$

and

$$c^+_{\alpha\gamma}(r) = 0, \qquad r > d \tag{2.18}$$

These are the equations we have solved and report upon in this paper.

When the molecules are reduced to a single site, or when all the sites become concentric (i.e., $L = 0$), this theory becomes identical to the Percus–Yevick-like theory of percolation put forth and solved analytically by Stratt and co-workers.[5] When both L and $\sigma = 0$, the theory coincides with that of Chiew and Glandt.[3] For nonzero L, Eqs. (2.16)–(2.18) pertain to a model with two additional lengths: σ, the hard-core diameter; and d, the connectivity diameter. Laria and Vericat employ RISM equations much like (2.16)–(2.18), but with a strength parameter ε in place of a

length σ. See Eq. (3.10) of ref. 13. It may be that their characterization is more appropriate than ours for soft colloidal suspension or micellar systems. But also their characterization may lack a systematic justification. Thus, we prefer the more straightforward modeling of excluded volume depicted in Eqs. (2.17) and (2.18).

2.4. Variational Solutions and Percolation

Our numerical work is facilitated by exploiting the variational procedure for solving RISM equations. This approach to computing $h_{\alpha\gamma}(r)$ and $c_{\alpha\gamma}(r)$ is well known.[22] We use it to solve Eqs. (2.11) with (2.15).

The corresponding variational equations we use for the connectivity functions are

$$\delta I^{+}_{\mathrm{RISM}}/\delta c^{+}_{\alpha\gamma}(r) = 0, \qquad r < d \tag{2.19}$$

where

$$\begin{aligned} I^{+}_{\mathrm{RISM}} = &-\sum_{\alpha,\gamma} \int d\mathbf{r}\, c^{+}_{\alpha\gamma}(r)[h_{\alpha\gamma}(r)+1] \\ &-[(2\pi)^3\rho^2]^{-1} \int d\mathbf{k}\, \{\mathrm{Tr}\, \rho\hat{\boldsymbol{\omega}}(k)\, \hat{\mathbf{c}}^{+}(k)] \\ &+\ln \det[\mathbf{1}-\rho\hat{\boldsymbol{\omega}}(k)\, \hat{\mathbf{c}}^{+}(k)]\} \end{aligned} \tag{2.20}$$

One may quickly verify that Eqs. (2.19) and (2.20) are indeed equivalent to Eqs. (2.16) and (2.17). According to Eq. (2.18), we need to determine $c^{+}_{\alpha\gamma}(r)$ only in the range $r < d$. Notice that according to Eq. (2.16), $c^{+}_{\alpha\gamma}(r)$ can be discontinuous at $r = \sigma$ and $r = d$, but continuous elsewhere. There can also be cusps at other values of r.[18] For each region in between these points of discontinuity and discontinuous derivative, we represent each $c^{+}_{\alpha\gamma}(r)$ as a polynomial in r. (Accounting for cusps is only of little importance in our numerical results, except for small L with large M.) The coefficients in these polynomials are then varied to minimize I^{+}_{RISM}.

As the percolation threshold is approached, the equations become more and more difficult to solve. Laria and Vericat[13] have noted this problem, too. The source of this difficulty is the physical divergence of S, which in the RISM theory is given by

$$S = \lim_{k \to 0} [\mathbf{1} - \rho\hat{\boldsymbol{\omega}}(k)\, \hat{\mathbf{c}}^{+}(k)]^{+1}_{\alpha\gamma} \tag{2.21}$$

This formula follows from Eqs. (2.2) and (2.16). In view of Eqs. (2.21) and (2.20), we see that the connectivity equations are well defined only for

$\rho \leqslant \rho_c$. As we increase the molecular density ρ toward ρ_c, we must decrease the incremental change in ρ to avoid artificial divergences in the Newton–Raphson cycles used to minimize I^+_{RISM}.

2.5. Reduced RISM Equations for Long Molecules

For large aspect ratios L/d, the number of interaction sites M becomes large. Since the number of site–site correlation functions scales as M^2, the straightforward application of the RISM equations can become intractable. On the other hand, most of the sites in the middle of a very long molecule should be approximately equivalent. By exploiting this equivalency, when it holds, the number of coupled RISM equations can be greatly reduced. This observation has been used to good effect by Chandler and co-workers[23] to treat the Feynman "polymers" representing quantal electrons. It has been used by Schweizer and Curro[24] and others (e.g., ref. 25) to treat real polymeric systems with RISM.

We have examined the possible equivalency in the direct connectedness functions calculated using the full set of topologically inequivalent sites. We find that for $L/d \gtrsim 10$, the sites in the interior of the rodlike molecule are well approximated as equivalent, while the two sites at the edges of the linear molecule should be treated differently until the molecules are much longer. Quantitative measures of the equivalency of the interior sites are presented in the Appendix. With only the interior and end sites treated as distinct, the $\mathbf{c}^+(r)$ matrix assumes the simple form

$$c^+_{\alpha\gamma}(r) = \begin{cases} c^+_{ee}(r), & \alpha, \gamma = 1 \text{ or } M \\ c^+_{ei}(r), & \alpha = 1 \text{ or } M, \quad 1 < \gamma < M \\ c^+_{ii}(r), & 1 < \alpha, \gamma < M \end{cases} \tag{2.22}$$

Similarly for $\mathbf{h}^+(r)$, $\mathbf{c}(r)$, and $\mathbf{h}(r)$. As a result, Eq. (2.16) yields

$$\begin{aligned} \hat{h}^+_{ee}(k) &= \{[\Delta\hat{\omega}(k)]^2\, \hat{c}^+_{ii}(k) + 2\hat{E}(k)\, \hat{\omega}_{ee}(k)\}/4\hat{D}(k) \\ \hat{h}^+_{ei} &= \{-[\Delta\hat{\omega}(k)]^2\, \hat{c}^+_{ei}(k) + 2\hat{E}(k)\, \hat{\omega}_{ei}(k)\}/2(M-2)\, \hat{D}(k) \\ \hat{h}^+_{ii}(k) &= \{[\Delta\hat{\omega}(k)]^2\, \hat{c}^+_{ee}(k) + \hat{E}(k)\, \hat{\omega}_{ii}(k)\}/(M-2)^2\, \hat{D}(k) \end{aligned} \tag{2.23}$$

where

$$\begin{aligned} \hat{D}(k) &= \det[\mathbf{1} - \rho\hat{\boldsymbol{\omega}}(k)\, \hat{\mathbf{c}}^+(k)] \\ &= 1 - \rho\hat{E}(k) \\ &= 1 - \rho\hat{T}(k) + \rho^2[\Delta\hat{\omega}(k)]^2\{[\hat{c}^+_{ei}(k)]^2 - \hat{c}^+_{ii}(k)\, \hat{c}^+_{ee}(k)\} \end{aligned} \tag{2.24}$$

$$\hat{T}(k) = \mathrm{Tr}\,\hat{\boldsymbol{\omega}}(k)\,\hat{\mathbf{c}}(k)$$
$$= 2\bar{\omega}_{ee}(k)\,\hat{c}^{+}_{ee}(k) + 4\bar{\omega}_{ei}(k)\,\hat{c}^{+}_{ei}(k) + \bar{\omega}_{ii}(k)\,\hat{c}^{+}_{ii}(k) \tag{2.25}$$

and

$$\Delta\hat{\omega}^2(k) = 4\bar{\omega}^2_{ie}(k) - 2\bar{\omega}_{ii}(k)\,\bar{\omega}_{ee}(k) \tag{2.26}$$

with

$$\bar{\omega}_{ie}(k) = \sum_{\alpha=2}^{M-1} \hat{\omega}_{1\alpha}(k)$$
$$\bar{\omega}_{ee}(k) = [1 + \hat{\omega}_{1N}(k)] \tag{2.27}$$
$$\bar{\omega}_{ii}(k) = \sum_{\alpha,\gamma=2}^{M-1} \hat{\omega}_{\alpha\gamma}(k)$$

Further, the variational functional, Eq. (2.20), is reduced with the aid of Eqs.(2.24) and (2.25).

The reduced RISM equations for $\mathbf{c}(r)$ and $\mathbf{h}(r)$ are identical to the corresponding Eqs. (2.23)–(2.27) for $\mathbf{c}^{+}(r)$ and $\mathbf{h}^{+}(r)$. For large enough M, the inequivalency of the end groups can be ignored with negligible effect. In that case, only one set of equations remain relating $c(r) = c_{ii}(r)$ to $h(r) = h_{ii}(r)$, and relating $c^{+}(r) = c^{+}_{ii}(r)$ to $h^{+}(r) = h^{+}_{ii}(r)$. For example, Eq. (2.11) then yields

$$\hat{h}(k) = \bar{\omega}^2(k)\,\hat{c}(k)/[1 - M\rho\bar{\omega}(k)\,\hat{c}(k)] \tag{2.28}$$

where

$$\bar{\omega}(k) = M^{-1} \sum_{\alpha,\gamma} \hat{\omega}_{\alpha\gamma}(k) \tag{2.29}$$

Equation (2.28) is the centerpiece of Schweizer and Curro's RISM theory of polymer melts (and blends, when the evident modification to mixtures is made).[24] The corresponding connectivity equation is

$$\hat{h}^{+}(k) = \bar{\omega}^2(k)\,\hat{c}^{+}(k)/[1 - M\rho\bar{\omega}(k)\,\hat{c}^{+}(k)] \tag{2.30}$$

3. RESULTS

The calculations we describe now emphasize the role of molecular shape on the percolation threshold. A given length-to-width ratio can be mimicked with a variable number of interaction sites. We have checked

that in our theory the results presented here are not significantly altered by the use of auxiliary sites. For example, when $L/d = L/2\sigma = 3$, our calculations with either $M = 6$ or 12 are virtually indistinguishable. The Appendix provides some more information along these lines. In the captions for each of the following figures, we identify the specific number of sites employed to arrive at the illustrated results.

The short-range behavior of $h_{ii}^{+}(r)$ is plotted in Fig. 2. The actual shape of $h_{ii}^{+}(r)$ is very sensitive to the length of the molecule, the proximity of percolation as measured by $\delta\rho = \rho_c - \rho$, and the hard-core size. Increasing the hard core dramatically reduces the probability that two sites are connected to one another on a short length scale. In contrast, the standard site–site correlation function $h_{ii}(r)$ is not very sensitive, as seen in Fig. 3. Notice, too, that unlike the case of flexible polymers,[24] the sites of a long rigid rod do not shield each other, and $h_{ii}(r)$ rises quickly from -1 as r is increased from the hard core. One does notice, however, that $h_{ii}(r)$ decreases with increasing L. Due to the low density of the percolation threshold and the plurality of length scales, there is no oscillatory structure in either $h_{ii}^{+}(r)$ or $h_{ii}(r)$. This result is in contrast to the case of simple spheres.[5]

The percolation threshold volume fraction

$$\rho_c^* = \rho_c v_M(d) \tag{3.1}$$

is plotted as a function of σ/d for various aspect ratios in Fig. 4. Here $v_M(d)$ is the volume of the percolating shell of the M-site molecule. [See

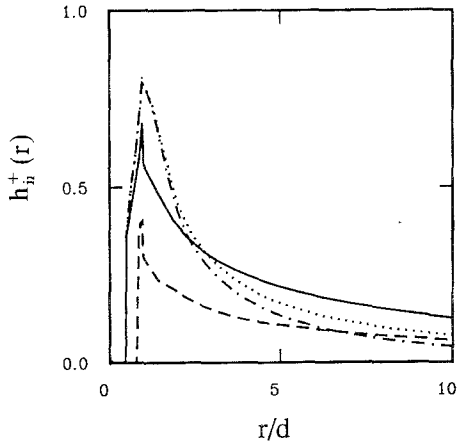

Fig. 2. The connectivity pair correlation function $h_{ii}^{+}(r)$ near the percolation threshold: $L/d = 1.5$, $M = 4$, $\delta\rho/\rho_c = 0.02$ (dotted line), and $\delta\rho/\rho_c = 0.1$ (dot-dashed line); for $L/d = 12.5$, $M = 26$, $\delta\rho/\rho_c = 0.01$ (solid line) and $\delta\rho/\rho_c = 0.01$, $M = 26$ (dashed line). σ/d is 0.5 in the first three cases and is 0.833 in the last one.

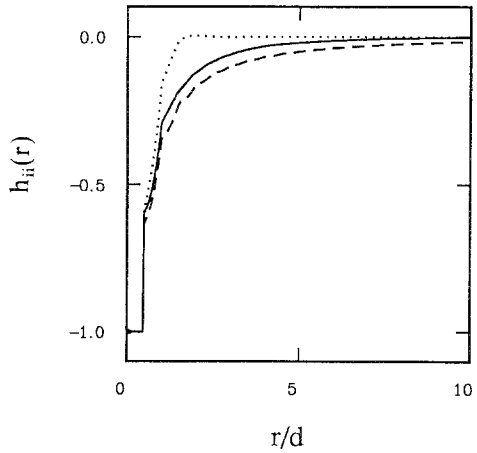

Fig. 3. The pair correlation function $h_{ii}(r)$ at the percolation threshold, $\rho = \rho_c$. From top to bottom: $L/d = 1.5$ ($M = 4$), 12.5 ($M = 26$), and 50 ($M = 101$). $\sigma/d = 0.5$ in all cases.

Eq. (3.1) of ref. 13.] For molecules with $L/d \leqslant 1.5$, our calculations predict reduced critical densities that reach a minimum at some intermediate value of σ and then increases sharply when σ approaches d. The $L = 0$ curve in that figure depicts the analytical results of Stratt and co-workers.[5] This is one limit of the RISM theory. At large aspect ratios, we predict that ρ_c^*

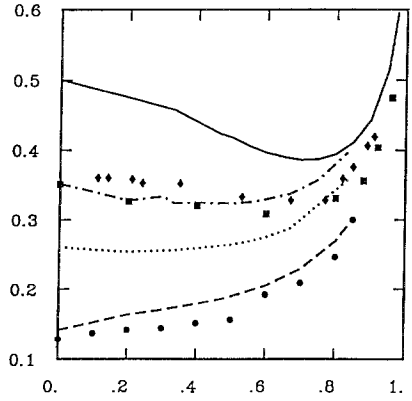

Fig. 4. The reduced percolation density at different aspect ratios. From top to bottom the lines are for $L/d = 0$ (ref. 5), 1.5, 2.5, and 5. The number of sites varies and does not affect the result obtained as long as the geometry is kept constant (see Appendix). The circles are Monte Carlo results for cylinders with $L/d = 5$ (ref. 26). The squares and diamonds are Monte Carlo results for $L/d = 0$ from refs. 10 and 11, respectively.

becomes almost constant for a large range of hard-core sizes. We have more to say about this later. The integral equation predictions at aspect ratio 5 are in reasonably good agreement with Monte Carlo results[26] for spherocylinders of the same length. For spheres, $L/d=0$, the agreement with Monte Carlo[10,11] is not as good, but it is still qualitatively reasonable. Lupowski and Monson[12] suggest that this approximate theoretical approach may improve in accuracy with increasing L/d; the comparisons in Fig. 4 may support their suggestion.

The nonmonotonic behavior shown in Fig. 4 for small aspect ratios is the result of two opposing features. First, increasing σ reduces the accessible volume of the outer percolating shell of the object, which in turn decreases the mean number of overlaps per molecule. Second, it increases the packing fraction of the fluid, thus forcing molecules together. The former tends to increase ρ_c^* and the latter decreases it. This competition makes ρ_c^* a nontrivial function of σ. The packing effect becomes negligible in the limit of zero density. Since increasing the length of the molecule causes percolation to occur at lower densities, the fact that ρ_c^* increases monotonically with σ for long molecules is not inconsistent with this argument.

Previous studies on the percolating behavior of long, totally permeable rods[16] suggest that, for such objects,

$$\rho_c^* \propto L^{-1}, \quad \text{or equivalently,} \quad \rho_c \sim M^{-2} \tag{3.2}$$

In Fig. 5 we examine this behavior at different hard-core sizes. Whereas

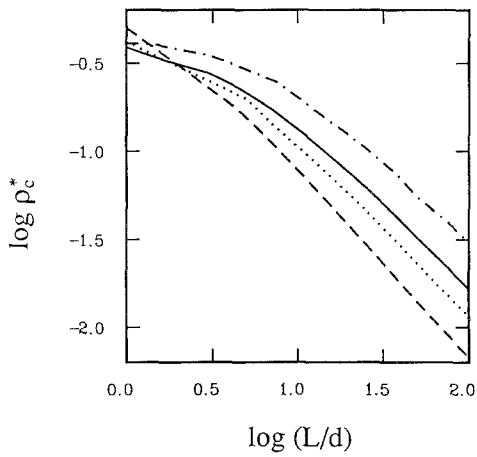

Fig. 5. ρ_c^* for different aspect ratios L/d at different hard-core sizes. From bottom to top: $\sigma/d=0$, 0.500, 0.667, and 0.833. The number of sites is adjusted so that intersite distance is equal to $d/2$.

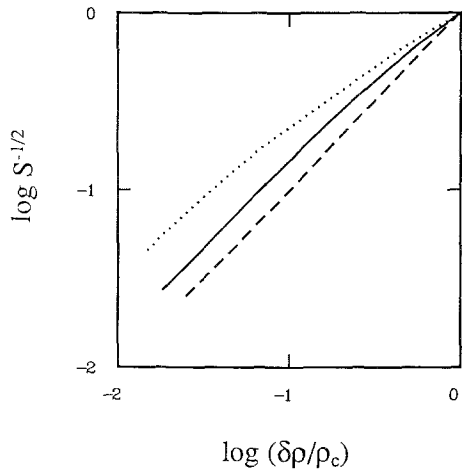

Fig. 6. $S^{-1/2}$ vs. $\delta\rho/\rho_c$ at $\sigma/d = 0.667$ at different aspect ratios. From top to bottom: $L/d = 50$ (101 sites), 12.5 (26 sites), and 1.5 (4 sites).

relation (3.2) seems true for totally permeable molecules starting at aspect ratio of around 5, it only begins to hold at larger aspect ratios as the hard-core size increases.

The critical exponents γ and ν are examined in Figs. 6 and 7, respectively. The analytical solution of the hard-sphere case $(L = 0)$[5] shows that for

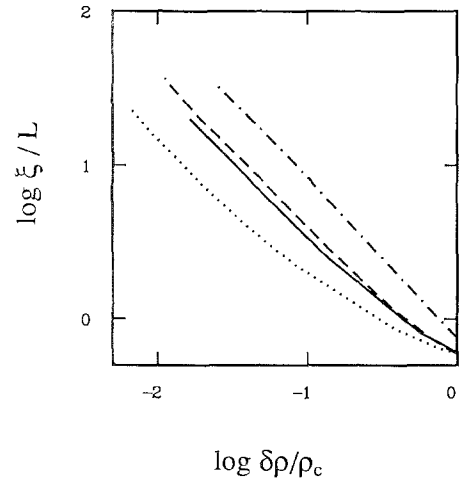

Fig. 7. ξ_{II}/L vs. $\delta\rho/\rho_c$. From top to bottom: $L/d = 1.5$ (computed with $M = 4$ sites), 12.5 (26 sites), 12.5 (26 sites), and 50 (101 sites). $\sigma/d = 0.667$ except for the dashed line, for which σ is zero.

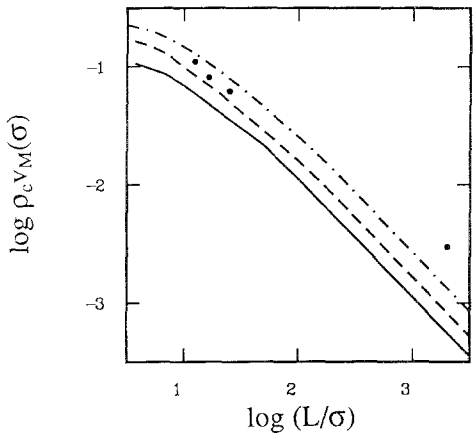

Fig. 8. Comparison between the experimentally obtained critical volume fraction (circles) to achieve conductivity at several aspect ratios (from Ref. 1) and percolation thresholds calculated with the present theory. The theoretical lines are, from top to bottom, $\sigma/d = 0.833$, 0.750, and 0.667. The number of sites used in the theoretical calculations is adjusted such that the intersite distance is less than 50% of σ in order to minimize the concavity of the molecules.

any $\sigma < d$, $\gamma = 2 = 2\nu$. Laria and Vericat[13] find $\gamma = 2$ analytically from the zero-pole approximation applied to permeable particles, $\sigma = 0$, at specific values of L/d. One expects to find these exponents from the RISM theory for any finite values of L, σ, and d, since for $\delta\rho$ small enough, the correlation length ξ is much larger than σ, d, or L. Indeed, this expectation of universality is borne out in Figs. 6 and 7. Notice also, however, that the range of densities for crossover from the limiting critical threshold behavior becomes more extended as L increases. We can analyze this behavior analytically as developed in the next section.

First, however, we turn to a limited comparison with experiment. These are conductivity studies[27] in which conductive fibers are randomly embedded in an insulating polymer. When the volume fraction of fibers is increased to a critical value, the dc conductivity experiences an increase of more than 10 orders of magnitude. In Fig. 8, we make a comparison between this critical volume fraction and the percolation threshold of "molecules" of the same aspect ratio. We use the connectivity diameter d as the only fitting parameter. More extensive experimental data of this type would be useful in testing this theory and analyzing the scaling for large L.

4. DISCUSSION

Let us now consider the critical scaling for very long molecules. For large enough M, we can neglect end effects and utilize the reduced RISM

equations, the connectivity counterparts to Eqs. (2.28) and (2.29). The qualitative behavior of $\bar{\omega}(k)$ is most significant. Figure 9 shows that for M large, the $\bar{\omega}(k)$ for different molecules are all relatively similar. For $k \lesssim 1/d$, we can capture the essential features with

$$\bar{\omega}(k) \approx (M-1)\frac{1}{1+\lambda^2 k^2} + 1 \tag{4.1}$$

where

$$\lambda/d \sim M \tag{4.2}$$

Equation (4.1) is correct for $k \ll 1/d$, the region of primary importance for critical phenomena. It also gives the correct $k \to \infty$ limit.

The function $\hat{c}^+(k)$ varies with k on a wavevector scale set by $1/d$, whereas $\bar{\omega}(k)$ varies most on the scale set by $1/Md$. Hence, for qualitative purposes, $\hat{c}^+(k)$ appearing in Eq. (2.30) can be replaced by

$$\begin{aligned} \hat{c}^+(k) &= c_0, \qquad k < k_c \\ &= 0, \qquad k \geqslant k_c \end{aligned} \tag{4.3}$$

where the cutoff wave vector can be taken as $k_c \approx 1/d$. In that case, the closure of the reduced RISM equation, Eq. (2.17), leads to

$$1 = \frac{1}{(2\pi)^2}\int_0^{1/d} dk\, \frac{k^2\bar{\omega}^2(k)c_0}{1 - M\rho\bar{\omega}(k)c_0} \tag{4.4}$$

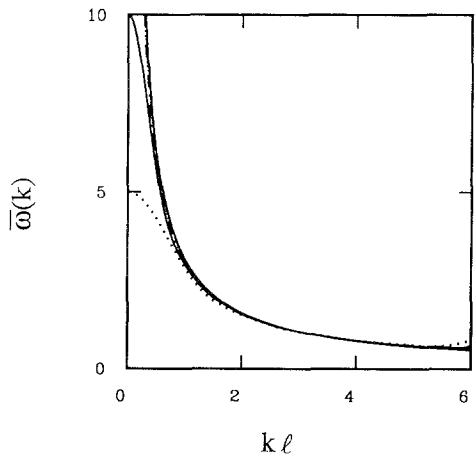

Fig. 9. The function $\bar{\omega}(k)$ versus k in units of inverse intersite distance l: $M = 5$ (dotted line); $M = 10$ (solid line). $\bar{\omega}(k)$ for $M = 20$, 30, 50, and 100 are indistinguishable in this region of k space on the scale of the graph.

To simplify the analysis with no significant effect on the end result, we have used on the left-hand side of Eq. (4.4) the constant associated with permeable percolating objects. In general, the left-hand side is a slowly varying density-dependent quantity. Equation (4.4) is to be solved for $c_0(\rho)$, and the exponent γ is determined from

$$S = [1 - \rho M^2 c_0(\rho)]^{-1} \sim (\delta\rho)^{-\gamma} \tag{4.5}$$

Assuming $c_0(\rho)$ is of order 1 and analytic near $\rho = \rho_c$, we can anticipate from Eq. (4.5) that $\rho_c d^3 \sim O(M^{-2})$ and that the exponent γ is a positive integer. Indeed, it is essentially with this argument that Bug *et al.*[16] concluded $\rho_c v_M \propto M^{-1}$ and that $\gamma = 1$. We agree with the first of their conclusions, but not the second.

By employing Eq. (4.1), one can perform the integral in Eq. (4.4) exactly, leading to a transcendental equation for $c_0(\rho)$. The equation can be simplified through expansions ordered in M^{-1} and in $(\rho_c - \rho)/\rho_c = \delta\rho/\rho_c$. Smallness of both these variables is required, of course, when invoking Eqs. (4.1)–(4.3). One finds from this analysis that

$$\rho_c = \frac{1}{6\pi^2 d^3} \frac{1}{M^2} [1 + O(M^{-1})] \tag{4.6}$$

Furthermore, if

$$\delta\rho/\rho_c \lesssim 1/M^2 \tag{4.7}$$

then

$$1 - \rho M^2 c_0(\rho) = (16/9\pi^2)\, M^2 (\delta\rho/\rho_c)^2 + \cdots \tag{4.8}$$

where the omitted subsequent terms are smaller by factors of M^{-1} and/or $(\delta\rho/\rho_c)$.

According to Eq. (4.6), as the molecules become longer, the threshold density decreases as M^{-2}. Furthermore, according to Eqs. (4.8) and (4.5), we have the critical exponent $\gamma = 2$. It is a possible "classical" exponent, but not the value of unity proposed by Bug *et al.*[16] Notice, however, that the asymptotic scaling of S does not hold until $\delta\rho/\rho_c$ is extremely small, Eq. (4.7). The prediction of $\gamma = 2$ should be compared with the best estimates of this exponent based upon Monte Carlo calculations[1,28]: $\gamma \approx 1.7$–1.8.

It is perhaps worth stressing that our use of the terminology "classical exponent" refers to the assumption of analyticity near the critical density. We do not assume a low-order truncation of a virial or low-density expansion. Such an assumption, which yields $\gamma = 1$, seems untenable in the

threshold region, where an infinite-order series is required to describe the percolating network.

One final remark concerns the correlation length critical exponent ν. It is clear from Eqs. (2.30) and (4.1) that the correlation function is analytic in k for small k. It follows that in this theory, $\xi^2 \sim S$. As a result, $\nu = \gamma/2 = 1$.

In conclusion, therefore, the RISM approach to continuum percolation is a classical theory which makes reasonable estimates of scaling and threshold densities. But neither is quantitatively accurate. Improvements along the lines proposed by Stell[4] for simple systems might be worthy of examination. Even without further improvements, however, possible extensions can be pursued immediately with only slight generalizations of what we have discussed in this paper. These extensions include studies of directed percolation relevant to "living" polymers, scaling and crossover behavior for systems of flexible polymers, and percolation in ordered fluids such as liquid crystals.

APPENDIX

Predictions of a consistent theory should be invariant to the addition of auxiliary sites so long as the molecular geometry is relatively unchanged. We have tested our calculations to be sure the results reported in the main text satisfy this criterion of consistency. In Fig. 10 the inverse mean cluster

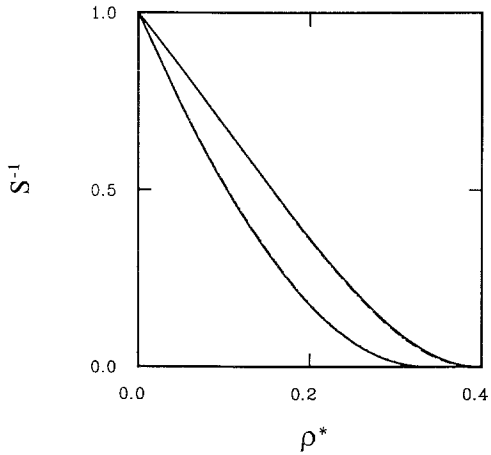

Fig. 10. $1/S$ vs. ρ^* at aspect ratio 1.5. Upper curves: $\sigma/d = 0.833$. Lower curves: $\sigma/d = 0.667$. The values of $1/S$ calculated with different numbers of auxiliary sites (four, five, and six) are barely distinguishable on the scale of the graph.

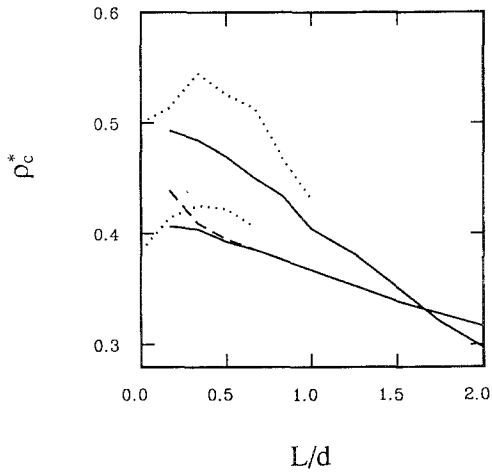

Fig. 11. ρ_c^* at short aspect ratios. The solid lines are obtained by using three or more sites and the dotted lines with two sites. Upper curves correspond to $\sigma/d = 0$; lower curves are for $\sigma/d = 0.667$. For example, the dashed line is calculated using four sites and differs slightly from the solid line, which is computed with three sites in that region.

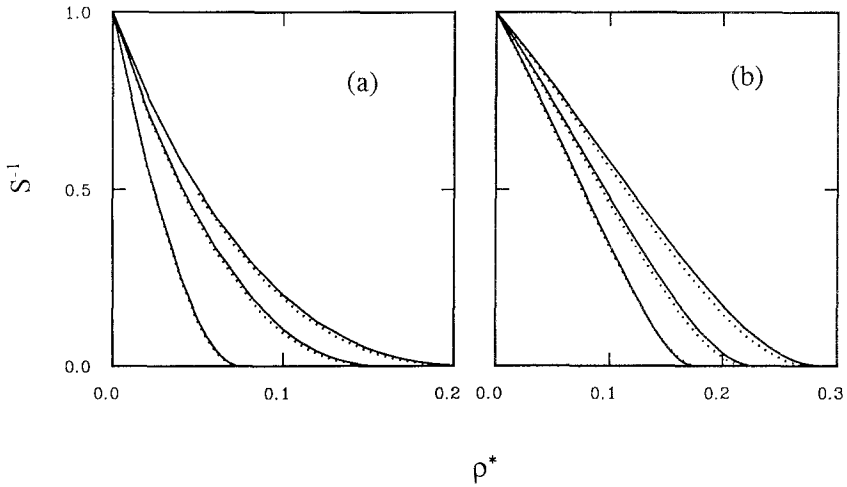

Fig. 12. $1/S$ computed with and without the assumption of equivalent interior sites. Solid lines are computed by setting all sites except the two end ones to be identical. Dotted lines are computed with the full set of inequivalent sites. (a) $\sigma/d = 0$, and the three curves from top to bottom refer to $M = 6$, 8, and 16. Intersite distances are kept at $0.667d$ in all cases. (b) $\sigma/d = 0.833$, and $M = 8$, 12, and 16 from top to bottom. Intersite distances are kept at $0.667d$ in the former two cases and $0.75d$ in the last one.

size is plotted against density. The phase diagram is unchanged whether one uses four, five, or six sites to represent the molecule. For short aspect ratios, such excellent agreement requires several more sites per unit length, as can be seen in Fig. 11. Many discontinuities in the basis functions are required for the very small-aspect-ratio calculations to ensure convergence. ρ_c^* is relatively independent of whether two or three sites per length d are used, except when the L/d ratio is less than 1; for $1/6 < L/d < 1$, one requires at least three or four sites per length d to obtain results invariant to the number of sites employed. Even more sites are required for smaller lengths. For $L = 0$ exactly, however, any number of sites is equivalent to one site, as is easily demonstrated formally from the RISM equations.

In addition to testing invariance to auxiliary sites, we have examined the quantitative accuracy of the reduced RISM equations which treat interior sites as equivalent. The tests are illustrated in Fig. 12. The graphs indicate that for molecules with $M > 6$ or $L/d \geqslant 5$, the reduced description is quite accurate.

ACKNOWLEDGMENTS

This research has been supported by the National Science Foundation and by the National Institute of Health.

We are grateful to Jerry Percus, whose work over the last four decades has motivated nearly all our ideas on integral equation theories of fluids.

REFERENCES

1. D. Stauffer, *Introduction to Percolation Theory* (Taylor & Francis, London, 1985); D. Stauffer, in *Percolation, Structures and Processes*, G. Deutscher, R. Zallen, and J. Adler, eds. (Adam Hilger, Bristol, England, 1983).
2. A. Coniglio, U. De Angelis, and A. Forlani, *J. Phys. A* **10**:1123 (1977).
3. Y. C. Chiew and E. D. Glandt, *J. Phys. A* **16**:2599 (1983).
4. Y. C. Chiew and G. Stell, *J. Chem. Phys.* **90**:4956 (1989); G. Stell, *J. Phys. A* **17**:L859 (1984).
5. T. DeSimone, S. Demoulini, and R. M. Stratt, *J. Chem. Phys.* **85**:391 (1986).
6. J. Xu and G. Stell, *J. Chem. Phys.* **89**:1101 (1988).
7. Y. C. Chiew, G. Stell, and E. D. Glandt, *J. Chem. Phys.* **83**:761 (1985).
8. J. K. Percus and G. J. Yevick, *Phys. Rev.* **110**:1 (1958); J. K. Percus, in *Equilibrium Theory of Classical Fluids*, H. L. Frisch and J. L. Lebowitz, eds. (Benjamin, New York, 1964).
9. E. M. Waisman, *Mol. Phys.* **25**:45 (1973).
10. S. A. Safran, I. Webman, and G. S. Grest, *Phys. Rev. Lett.* **55**:1896 (1985).
11. J. G. Saven, J. L. Skinner, and J. R. Wright, *J. Chem. Phys.* (1991).
12. M. Lupkowski and P. A. Monson, *J. Chem. Phys.* **89**:3300 (1988).
13. D. Laria and F. Vericat, *Phys. Rev. B* **40**:353 (1989).

14. D. Chandler, in *Studies in Statistical Mechanics VIII*, E. W. Montroll and J. L. Lebowitz, eds. (North-Holland, Amsterdam, 1982), p. 275; and P. A. Monson and G. P. Morriss, *Adv. Chem. Phys.* **77**:451 (1990).
15. D. Chandler, J. D. Weeks, and H. C. Andersen, *Science* **220**:787 (1983).
16. I. Balberg, N. Binenbaum, and N. Wagner, *Phys. Rev. Lett.* **52**:1465 (1984); I. Balberg, C. H. Anderson, S. Alexander, and N. Wagner, *Phys. Rev. B* **30**:3833 (1984); A. L. R. Bug, S. A. Safran, and I. Webman, *Phys. Rev. B* **33**:4716 (1986).
17. T. L. Hill, *J. Chem. Phys.* **23**:617 (1955); T. L. Hill, *Introduction to Statistical Thermodynamics* (Addison-Wesley, Reading, Massachusetts, 1960).
18. B. M. Ladanyi and D. Chandler, *J. Chem. Phys.* **62**:4308 (1975).
19. D. Chandler and L. R. Pratt, *J. Chem. Phys.* **65**:2925 (1976); L. R. Pratt and D. Chandler, *J. Chem. Phys.* **66**:147 (1977).
20. D. Chandler and H. C. Andersen, *J. Chem. Phys.* **57**:1930 (1972).
21. D. Chandler, *Mol. Phys.* **31**:1213 (1976).
22. L. J. Lowden, RISM, RISMGR, RISMSK: Program Number QCPE 306, Quantum Chemistry Program Exchange, Indiana University, Bloomington, Indiana 47401.
23. D. Chandler, Y. Singh, and D. M. Richardson, *J. Chem. Phys.* **81**:1975 (1984); D. Chandler, *Chem. Phys. Lett.* **139**:108 (1987).
24. K. S. Schweizer and J. G. Curro, *Chem. Phys.* **149**:105 (1990), and references cited therein.
25. F. Hirata and R. M. Levy, *J. Phys. Chem.* **93**:479 (1989).
26. I. Balberg and N. Binenbaum, *Phys. Rev. A* **35**:5174 (1987).
27. D. M. Bigg, *Polym. Eng. Sci.* **19**:1188 (1979).
28. I. Balberg, *Phil. Mag.* **56**:991 (1987).